OPEN

Citation: Cell Death and Disease (2013) 4, e563; doi:10.1038/cddis.2013.94

www.nature.com/cddis

Netrin-1 protects hypoxia-induced mitochondrial apoptosis through HSP27 expression via DCC- and integrin $\alpha6\beta4$-dependent Akt, GSK-3β, and HSF-1 in mesenchymal stem cells

TW Son[1,4], SP Yun[2,4], MS Yong[2], BN Seo[2], JM Ryu[2], HY Youn[1], YM Oh[3] and HJ Han*[,2]

Netrin (Ntn) has the potential to be successfully applied as an anti-apoptotic agent with a high affinity for tissue, for therapeutic strategies of umbilical cord blood-derived mesenchymal stem cells (UCB-MSC), although the mechanism by which Ntn-1 protects hypoxic injury has yet to be identified. Therefore, the present study examined the effect of Ntn-1 on hypoxia-induced UCB-MSC apoptosis, as well as the potential underlying mechanisms of its protective effect. Hypoxia (72 h) reduced cell viability (MTT reduction, and [^{3}H]-thymidine incorporation) and cell number, and induced apoptosis (annexin and/or PI positive), which were reversed by Ntn-1 (10 ng/ml). Moreover, Ntn-1 decreased the increase of hypoxia-induced Bax, cleaved caspase-9, and -3, but blocked the decrease of hypoxia-reduced Bcl-2. Next, in order to examine the Ntn-1-related signaling cascade in the protection of hypoxic injury, we analyzed six Ntn receptors in UCB-MSC. We identified deleted in colorectal cancer (DCC) and integrin (IN) $\alpha6\beta4$, except uncoordinated family member (UNC) 5A–C, and neogenin. Among them, IN $\alpha6\beta4$ only was detected in lipid raft fractions. In addition, Ntn-1 induced the dissociation of DCC and APPL-1 complex, thereby stimulating the formation of APPL-1 and Akt2 complex. Ntn-1 also reversed the hypoxia-induced decrease of Akt and glycogen synthase kinase 3β (GSK-3β) phosphorylation, which is involved in heat shock factor-1 (HSF-1) expression. Ntn-1-induced phospho-Akt and -GSK-3β were inhibited by DCC function-blocking antibody, IN a6b4 function-blocking antibody, and the Akt inhibitor. Hypoxia and/or Ntn-1 stimulated heat shock protein (HSP)27 expression, which was blocked by *HSF-1*-specific small interfering RNA (siRNA). Furthermore, *HSP27*-specific siRNA reversed the Ntn-1-induced increase of phospho-Akt. Additionally, *HSP27*-specific siRNA attenuated the Ntn-1-reduced loss of mitochondrial membrane injury via the inhibition of cytochrome *c* (cyt *c*) release and formation of cyt *c* and HSP27 complex. Moreover, the inhibition of each signaling protein attenuated Ntn-1-induced blockage of apoptosis. In conclusion, Ntn-1-induced HSP27 protected hypoxic injury-related UCB-MSC apoptosis through DCC- and IN $\alpha6\beta4$-dependent Akt, GSK-3β, and HSF-1 signaling pathways.

Cell Death and Disease (2013) **4,** e563; doi:10.1038/cddis.2013.94; published online 28 March 2013
Subject Category: Experimental Medicine

Human mesenchymal stem cells (hMSCs) have distinct characteristics, with a self-renewal capacity and the ability to generate multiple differentiated cell types.[1] Therefore, hMSCs have been targeted in the field of developmental biology and used in a vast number of therapeutic applications.[2] Although several studies involving clinical applications have detailed MSC transplantation and/or therapeutic methods,[3] the serious problem of hypoxic injury may arise during transplantation and cell therapy.[4] Interestingly, alteration of the duration of hypoxic conditions (oxygen concentrations $<2\%$) has been shown to have a contrasting role in stem cells (SCs). In a short period of time (under 48 h), hypoxia induced the proliferation, migration, and differentiation of various SCs, including MSCs.[5,6] Additionally, over a longer period of time (>72 h), hypoxia can reduce SC proliferation and/or lead to programmed cell death.[7] In respect of SC therapy or

[1]Department of Veterinary Internal Medicine, College of Veterinary Medicine and Research Institute for Veterinary Science, Seoul National University, Seoul, Korea; [2]Department of Veterinary Physiology, College of Veterinary Medicine and Research Institute for Veterinary Science, Seoul National University, Seoul, Korea and [3]Department of Pulmonary and Critical Care Medicine, and Clinical Research Center for Chronic Obstructive Airway Diseases, Asan Medical Center, University of Ulsan College of Medicine, Seoul, Korea
*Corresponding author: HJ Han, Department of Veterinary Physiology, College of Veterinary Medicine and Research Institute for Veterinary Science, Seoul National University, Seoul 151-741, Korea. Tel: 82 2 880 1261; Fax: 82 2 885 2732; E-mail: hjhan@snu.ac.kr
[4]These authors contributed equally to this work.
Keywords: umbilical cord blood-derived mesenchymal stem cell; netrin-1; hypoxic injury; apoptosis; cytoprotection; heat shock protein
Abbreviations: Ab, antibody; APPL, an adapter protein containing a pleckstrin homology domain, a PTB domain, and a leucine zipper motif; Bax, Bcl-2-associated X protein; Bcl-2, B-cell lymphoma 2; Cav, caveolin; cyt *c*, cytochrome *c*; DCC, deleted in colorectal cancer; FACS, fluorescence-activated cell sorter; FBS, fetal bovine serum; GSK-3β, glycogen synthase kinase 3β; HSF, heat shock factor; HSP, heat shock protein; IN, integrin; IP, immunoprecipitation; MTT, 3-(4,5,-dimethyl thiazolyl-2)-2,5-diphenyl tetrazolium bromide; NAC, *N*-acetylcysteine; Ntn, netrin; PBS, phosphate-buffered saline; PI, propidium iodide; PI3K, phosphatidylinositol 3-kinases; PVDF, polyvinylidene fluoride; ROD, relative optical density; RT-PCR, reverse transcription-polymerase chain reaction; SC, stem cell; SE, standard errors; siRNA, small interfering ribonucleic acid; TBST, tris-buffer solution-Tween-20; TCA, trichloroacetic acid; UCB-MSC, umbilical cord blood-derived mesenchymal stem cell; UNC, uncoordinated family member
Received 10.11.12; revised 31.1.13; accepted 14.2.13; Edited by Y Shi

transplantation, although short-term hypoxic conditions stimulated SC viability, injected or transplanted SCs underwent long-term hypoxic conditions, and subsequent long-term hypoxic conditions were the leading causes of cell death. Thus, it is important to illuminate tissue-affinitive protective factors of hypoxic injury in order to apply MSC to regeneration strategies, and therefore, its mechanisms of controlling hypoxia-mediated MSC apoptosis must be understood in detail.

Netrin (Ntn), an evolutional conserved family of laminin-related protein, is a multifunctional guidance molecule that serves as a regulatory factor of cell apoptosis, morphogenesis, and invasion.[8] With respect to apoptosis, Ntn-1 has been introduced as an anti-apoptotic agent against hypoxic injury of the brain tissue.[9,10] Therefore, it is possible that Ntn-1 in the extracellular plasma environment may be involved in a protective capacity against hypoxia-induced UCB-MSC (umbilical cord blood-derived mesenchymal stem cell) apoptosis. Recent findings have implicated Ntn in the regulation of adult SC migration, tumor cell survival, and embryonic development, suggesting potentially novel means of promoting recovery from cellular injury and achieving improvements in tissue regeneration.[11–13] In addition, Ntn is crucial to maintain the survival of Ntn-receptor-expressed cells during tissue development.[14] In this regard, Ntn, Ntn receptors, and the associated downstream signaling mechanisms involved are promising targets for the prevention of extracellular damage. However, there are no previous reports related to anti-apoptotic effects of tissue-affinitive Ntn-1 in UCB-MSCs for regeneration strategies. We assume that exogenous and tissue-affinitive Ntn-1 can prevent cell death from extracellular damage, and improve subsequent survival. If so, Ntn, Ntn receptors, and the downstream signaling mechanisms involved are promising targets for the prevention for extracellular damages. Thus, determining how Ntn receptors and signal transduction proteins function as an ensemble in regulating apoptosis remains a major challenge for current studies. Therefore, the present study examined the effect of Ntn-1 on hypoxia-induced UCB-MSC apoptosis and its related signal pathways.

Results

Effect of Ntn-1 on hypoxia-induced UCB-MSC apoptosis via lipid raft-independent DCC and -dependent IN $\alpha6\beta4$. To ensure that the hypoxic condition (2.2% O_2, 5.5% CO_2, and 92.3% N_2) used in this study induces typical cell apoptosis in UCB-MSCs, the cells were exposed to hypoxic conditions for various periods (0–72 h). MTT reduction levels and [^{3}H]-thymidine incorporation levels were increased until 48 h of hypoxic conditions, but significantly decreased after 72 h (Figures 1a and b). To investigate the protective effect of Ntn-1 on hypoxic injury, cells were pretreated with Ntn-1 (10 ng/ml) for 72 h. Pretreatment of Ntn-1 reversed hypoxia-reduced MTT reduction levels and [^{3}H]-thymidine incorporation levels (Figures 1c and d). To further elucidate the hypoxia-induced UCB-MSC apoptosis and anti-apoptotic effects of Ntn-1, each of these was assessed using cell number counting, cell viability assay, and annexin V/PI apoptosis assay. These results showed that exposure to hypoxia for 72 h increased the apoptotic cell death, which was blocked by Ntn-1 (Figures 1e–g). Consistent with these results, hypoxia increased Bcl-2-associated X protein (Bax), cleaved caspase-9, and cleaved caspase-3, but decreased B-cell lymphoma 2 (Bcl-2) expression, which was reversed by Ntn-1 (Figures 1h and i). In experiments to compare efficacy of the anti-apoptotic effect, Ntn-1, *N*-acetylcysteine (NAC, 1 mM), and ascorbic acid (1 μM) were determined to have similar effects (Supplementary Figure 1).

In order to examine the mechanism of Ntn-1 effects, we first determined the existence of Ntn receptors, such as those deleted in colorectal cancer (DCC), uncoordinated family member (UNC) 5, neogenin, and integrin (IN) $\alpha6\beta4$, along with their function on hypoxia-induced UCB-MSC apoptosis. As shown in Figures 2a and b, we detected DCC and IN $\alpha6\beta4$, but did not find UNC5A, UNC5B, UNC5C, or neogenin. Moreover, DCC and IN $\alpha6\beta4$ expressions were not changed by Ntn-1 or hypoxia. To further elucidate the localization of DCC and IN $\alpha6\beta4$, they were each assessed using immunoprecipitation and discontinuous sucrose density-gradient centrifugation. DCC did not colocalize with IN $\alpha6\beta4$, and IN $\alpha6\beta4$ localized in the lipid raft fraction, but not DCC (Figures 2c and d). In addition, pretreatment of DCC or IN $\alpha6\beta4$ with function-blocking antibody inhibited an Ntn-1-induced decrease of Bax and an increase of Bcl-2 (Figures 2e and f). These results suggest that the protective effect of Ntn-1 on hypoxia-induced UCB-MSC apoptosis is mediated by lipid raft-independent DCC and -dependent IN $\alpha6\beta4$.

Effect of Ntn-1 on DCC-related anti-apoptotic protein complex, Akt, GSK-3β, and HSF-1. A cytoprotective effect of Ntn-1 is thought to occur through various signal pathways. Thus, we examined whether or not Ntn-1 has a role in regulating DCC-dependent signal pathways, including those of DCC/caspase-3, DCC/APPL-1, and APPL-1/Akt2 complexes. As shown in Figure 3a, the DCC/caspase-3 complex existed in normal UCB-MSCs, but was not changed by hypoxic conditions, with or without pretreatment with Ntn-1. However, Ntn-1 increased the dissociation of DCC/APPL-1 complex, which was blocked by DCC function-blocking antibody (Figure 3b). Moreover, the formation of APPL-1/Akt2 complex was increased by Ntn-1 (Figure 3c). Next, we examined Akt phosphorylation, which is generally well known as a key molecule in the survival pathway. The phosphorylation of Akt^{thr308} and Akt^{ser473} was decreased after 72 h incubation under hypoxic conditions, whereby Ntn-1 reversed Akt^{thr308} and Akt^{ser473} phosphorylation, which was blocked by DCC and IN $\alpha6\beta4$ function-blocking antibody (Figures 3d and e).

To examine whether or not Ntn-1 has a role in the regulation of Akt-related glycogen synthase kinase-3β (GSK-3β) phosphorylation and heat shock factor-1 (HSF-1) expression, we assessed whether Ntn-1 induces GSK-3β phosphorylation and HSF-1 expression. As shown in Figures 4a and b, Ntn-1 reversed the hypoxia-induced decrease of GSK-3β phosphorylation, which was blocked by Akt inhibitor. In addition, GSK-3β inhibitor lithium chloride (LiCl) and Ntn-1 significantly increased HSF-1 levels in both the non-nuclear and nuclear fractions, confirming that the increase of HSF-1 results from GSK-3β phosphorylation (Figure 4c).

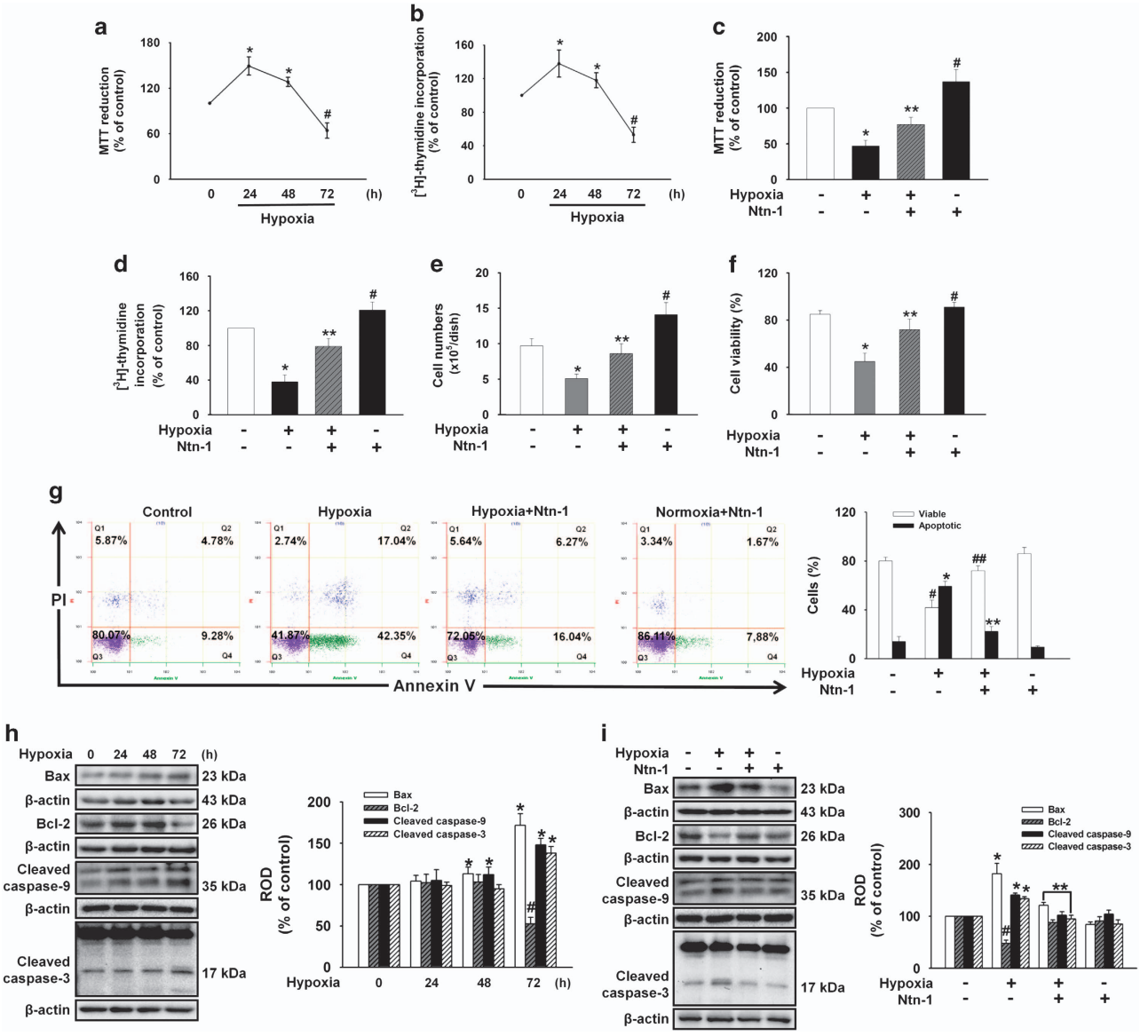

Figure 1 Effect of Ntn-1 on hypoxia-induced UCB-MSC apoptosis. (**a**) Cells were exposed to hypoxia for 0–72 h and analyzed for their viability by MTT assay. The values are reported as a mean ± S.E. of three independent experiments with triplicate dishes. $^{*,\#}P<0.05$ *versus* control. (**b**) Cells were exposed to hypoxia for 0–72 h and pulsed with 1 μCi of [^{3}H]-thymidine for 1 h prior to counting. The values are reported as a mean ± S.E. of three independent experiments with triplicate dishes. $^{*,\#}P<0.05$ *versus* control. (**c**) Cells were pretreated with Ntn-1 (10 ng/ml) for 30 min before being exposed to hypoxia for 72 h, and analyzed for their viability by MTT assay. The values are reported as mean ± S.E. of three independent experiments with triplicate dishes. $^{*,\#}P<0.05$ *versus* control, $^{**}P<0.05$ *versus* hypoxia alone. (**d**) Cells were pretreated with Ntn-1 for 30 min before being exposed to hypoxia for 72 h, and then pulsed with 1 μCi of [^{3}H]-thymidine for 1 h prior to counting. The values are reported as mean ± S.E. of three independent experiments with triplicate dishes. $^{*,\#}P<0.05$ *versus* control, $^{**}P<0.05$ *versus* hypoxia alone. (**e** and **f**) Cells were pretreated with Ntn-1 (10 ng/ml) for 30 min before being exposed to hypoxia for 72 h, and the number of cells and viability was determined using a Countess automated cell counter. The values represent mean ± S.E. of five independent experiments with triplicate dishes. $^{*,\#}P<0.05$ *versus* control, $^{**}P<0.05$ *versus* hypoxia alone. (**g**) Cells were pretreated with Ntn-1 (10 ng/ml) for 30 min before being exposed to hypoxia for 72 h. The cells were washed with PBS, stained, and analyzed by flow cytometry. Survival and apoptosis was measured using annexin V/PI staining and flow cytometry. Annexin V/PI double negative cells (Q3) were considered alive, annexin V positive/PI-negative cells (Q4) were considered early apoptotic, and annexin V/PI double-positive cells (Q2) were considered late apoptotic. One representative experiment out of three is shown (left column). Quantitative analysis of the percentage of viable or apoptotic cells by FACS analysis (right column). $^{*,\#}P<0.05$ *versus* control, $^{**,\#\#}P<0.05$ *versus* hypoxia alone. (**h**) Cells were exposed to hypoxia for 0–72 h, and Bax, Bcl-2, caspase-9, and caspase-3 were detected by western blot. Each example shown is representative of five experiments. (**i**) Cells were pretreated with Ntn-1 for 30 min before being exposed to hypoxia for 72 h, and Bax, Bcl-2, caspase-9 and caspase-3 were detected by western blot. Each example shown is representative of five experiments. The right part (**h** and **i**) depicting the bars denotes the mean ± S.E. of five independent experiments for each condition determined from densitometry relative to β-actin. $^{*,\#}P<0.05$ *versus* control, $^{**}P<0.05$ *versus* hypoxia alone. ROD, relative optical density

Role of heat shock protein 27 (HSP27) and Ntn-1-related signaling proteins in Ntn-1-in the induced cytoprotective effects. Heat shock protein (HSP) isoforms in Ntn-1-induced cytoprotective effects were determined. In order to determine the HSP isoform expression by hypoxia and/or Ntn-1, we determined variations in HSP27, HSP60, HSP70, and

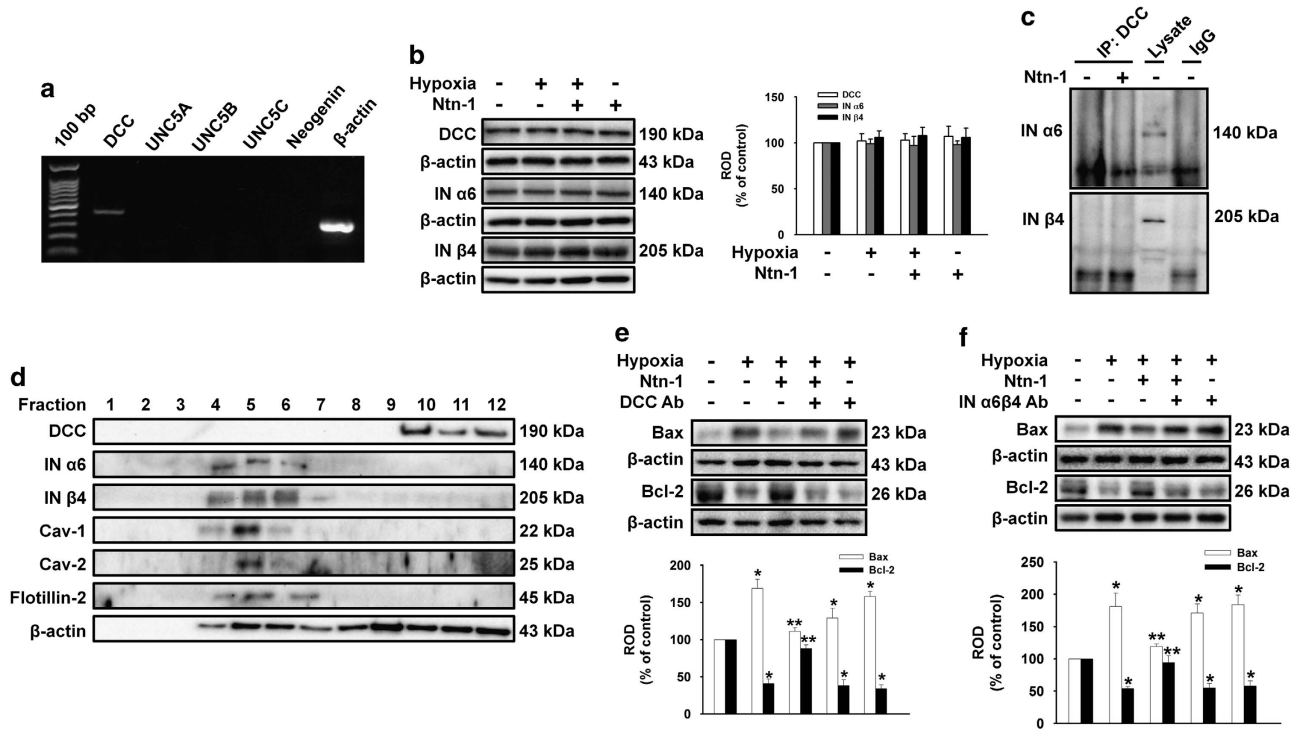

Figure 2 Protective effect of Ntn-1 on hypoxia-induced UCB-MSC apoptosis via DCC and IN $\alpha6\beta4$. (**a**) Total RNA from UCB-MSCs was reverse transcribed, and *DCC*, *UNC5A*, *UNC5B*, *UNC5C*, and *neogenin* cDNA were amplified by PCR, as described in Materials and Methods. Each example shown is representative of five independent experiments. (**b**) Cells were pretreated with Ntn-1 (10 ng/ml) for 30 min before being exposed to hypoxia for 72 h, and DCC, IN $\alpha6$, and IN $\beta4$ were detected by western blot. (**c**) Cells were incubated in the presence of Ntn-1 for 24 h and then harvested. Cell lysates were analyzed by western blotting with antibodies to INs $\alpha6$ and $\beta4$. Anti-DCC immunoprecipitation was analyzed by western blotting with INs $\alpha6$ and $\beta4$ antibodies. (**d**) Control lysate was subjected to discontinuous sucrose density-gradient fractionation, after which DCC, IN $\alpha6$, IN $\beta4$, caveolin (Cav)-1, Cav-2, flotillin-2, and β-actin were detected. Each fraction was assessed by western blot. (**e** and **f**) Cells were pretreated with DCC function-blocking antibody (2.5 μl/ml) or combination of INs $\alpha6$ and $\beta4$ function-blocking antibodies (2.5 μl/ml) for 30 min prior to hypoxia with Ntn-1 exposure for 72 h; Bax and Bcl-2 were detected by western blot. (**b**–**f**) Each example shown is representative of five experiments. The lower or right part (**b**, **e** and **f**) depicting the bars denotes the mean ± S.E. of five independent experiments for each condition determined from densitometry relative to β-actin. $^*P<0.05$ *versus* control, $^{**}P<0.05$ *versus* hypoxia alone. ROD, relative optical density

HSP90 expression under treatment conditions. As shown in Figure 5a, HSP27 expression was increased by hypoxia and/or Ntn-1, but not HSP60, HSP70, and HSP90. In addition, pretreatment of *HSF-1*-specific small interfering RNA (siRNA) inhibited Ntn-1-indcued HSP27 expression (Figure 5b). As shown in Figure 5c, Ntn-1 reversed the hypoxia-induced decrease of Akt^{thr308} and Akt^{ser473} phosphorylation, which were blocked by *HSP27*-specific siRNA. The Ntn-1-induced decrease of Bax was blocked by Akt inhibitor in the cytosolic and mitochondrial fractions (Figure 5d). Moreover, Ntn-1 reversed hypoxia-induced mitochondrial dysfunction and increase of cytochrome complex (cyt *c*) release, which were inhibited by *HSP27*-specific siRNA (Figures 5e and f). To further determine the specificity of the HSP27 and cyt *c* complex formation, cell lysates were immunoprecipitated with the anti-cyt *c* antibody, and were then immunoblotted with an anti-HSP27 or an anti-HSP70 antibody. These experiments confirmed that cyt *c* could interact with HSP27, but not HSP70 (Figure 5g). Moreover, *HSP27*-specific siRNA inhibited the Ntn-1-induced increase of HSP27 and cyt *c* complex, but did not change cyt *c* expression in cell lysates (Figure 5h).

To investigate the involvement of DCC, IN $\alpha6\beta4$, Akt, HSF-1, HSP27, and HSP70 in the protection of hypoxic injury by Ntn-1, UCB-MSCs were pretreated with DCC and IN $\alpha6\beta4$ function-blocking antibodies, a combination of DCC and IN $\alpha6\beta4$ function-blocking antibody, Akt inhibitor, *HSF-1*-, *HSP27*-, *HSP70*-, and *nontarget*-specific siRNA, prior to incubation for 72 h in hypoxic conditions both with/without Ntn-1. As shown in Figures 6a and b, pretreatment of DCC and IN $\alpha6\beta4$ function-blocking antibodies, the combination of DCC and IN $\alpha6\beta4$ function-blocking antibody, Akt inhibitor, *HSF-1*-, and *HSP27*-specific siRNA decreased the Ntn-1-induced increase of MTT reduction level, and [^{3}H]-thymidine incorporation level. In addition, these treatments blocked Ntn-1-induced reduction of annexin V and/or PI-positive cells, whereas *HSP70*-specific siRNA did not (Figure 6c).

Discussion

The results of the present study demonstrate that Ntn-1 effectively protects UCB-MSCs from hypoxia injury through the inhibition of mitochondrial dysfunction via HSP27 expression through lipid raft-independent DCC- and lipid raft-dependent IN $\alpha6\beta4$-mediated Akt/GSK-3β/HSF-1. Thus, our findings strongly suggested that Ntn-1 is a good candidate protective agent of hypoxic injury during cell transplantation and cell therapy. Ntn-1 has broad functions and regulates

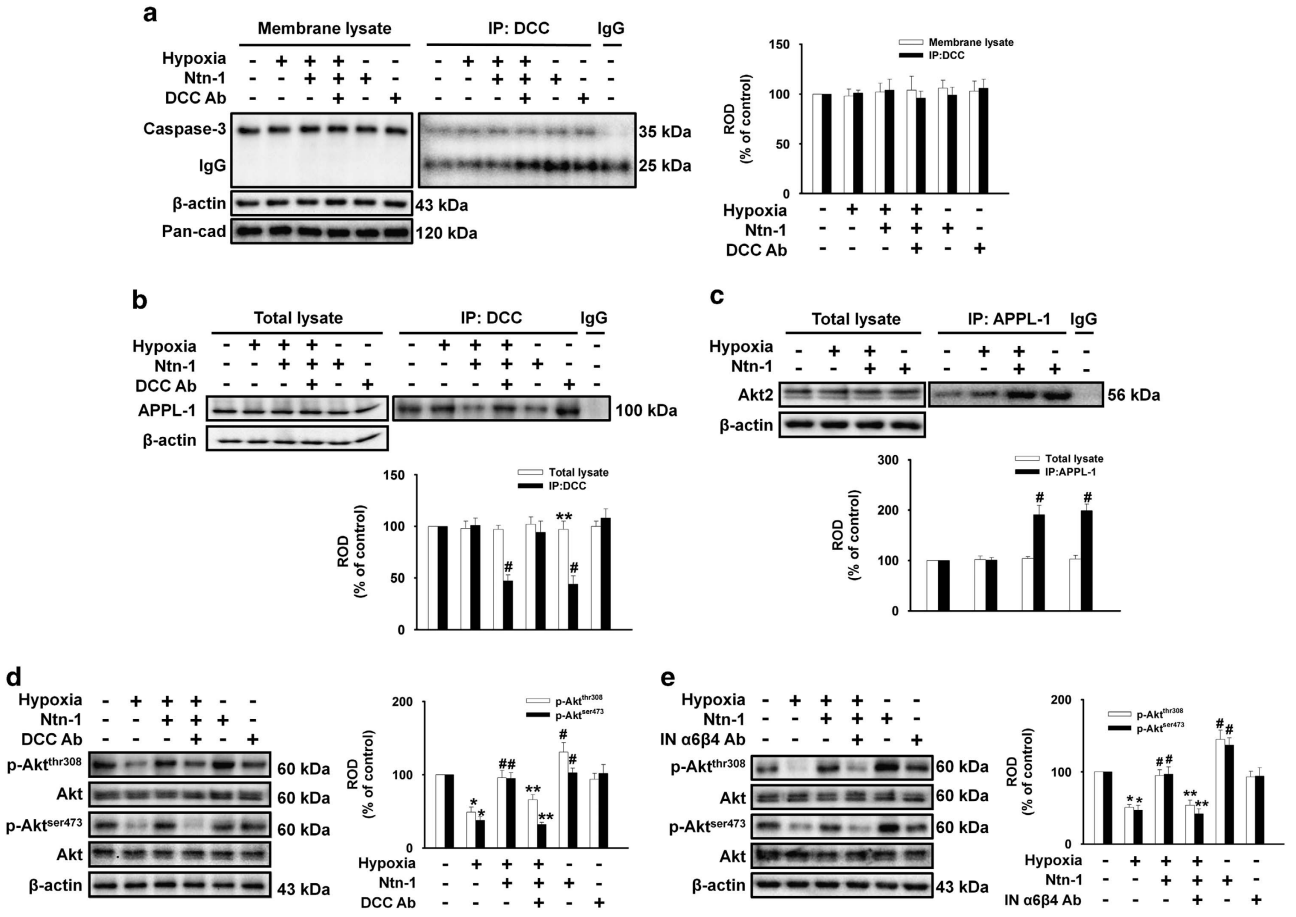

Figure 3 Involvement of DCC/caspase-3, APPL-1/Akt2 complexes and Akt phosphorylation. (**a** and **b**) Cells were pretreated with Ntn-1 (10 ng/ml) or DCC function-blocking antibody (2.5 μl/ml) for 30 min prior to 72 h incubation in hypoxic condition. Cell lysates were analyzed by western blotting with antibodies that recognize caspase-3 or APPL-1. Immunoprecipitation of anti-DCC was analyzed by western blotting with antibodies that recognize caspase-3 or APPL-1. (**c**) Cells were pretreated with Ntn-1 (10 ng/ml) for 30 min prior to 72 h incubation in hypoxic condition. Cell lysates were analyzed by western blotting with antibody that recognize Akt2. Immunoprecipitation of anti-APPL-1 was analyzed by western blotting with antibody that recognize Akt2. (**d** and **e**) Cells were pretreated with DCC function-blocking antibody (2.5 μl/ml), or combination of INs α6 and β4 (2.5 μl/ml) for 30 min prior to a 30-min Ntn-1 (10 ng/ml) treatment. And then, the cell incubated prior to 72 h in hypoxic condition. Total protein was extracted and blotted with phospho-Akt^{thr308}, phospho-Akt^{ser473}, or Akt antibody. (**a**–**e**) Each of the examples is representative of four independent experiments. The right or lower part (**a**–**e**) depicting the bars denotes the mean ± S.E. of four independent experiments for each condition determined from densitometry relative to β-actin or total Akt. $^{*}P<0.05$ *versus* control, $^{\#}P<0.05$ *versus* hypoxia alone, $^{**}P<0.05$ *versus* combination of hypoxia and Ntn-1. ROD, relative optical density

many biological processes, including cell proliferation, differentiation, and the determination of cell fate,[13,15,16] although Ntn-1 was originally thought to participate in the formation of axon.[8] These effects of Ntn-1 are dependent on the specificity of their interaction with different types of receptors, such as DCC, UNC5, neogenin, and INs, and the cell types in which they are differentially expressed.[17–19] Moreover, recent studies have demonstrated that the expression of these receptors takes place in embryos and SCs, suggesting the influence of Ntn on morphogenesis, development, and proliferation of SCs.[20–22] In this study, we found that DCC and IN $\alpha6\beta4$ existed in UCB-MSC, but UNC5 and neogenin were not found. Moreover, DCC and IN $\alpha6\beta4$ are required in lipid rafts for Ntn-1 function, and may initiate various anti-apoptotic signaling transduction, and regulate early embryonic development.[23–26] However, according to our data, IN $\alpha6\beta4$ was located in the lipid raft, but not in the DCC in UCB-MSCs. We also found that Ntn-1 effectively protects cells from hypoxia-induced UCB-MSC apoptosis, which was inhibited by DCC- and IN $\alpha6\beta4$-function-blocking antibodies. Although lipid raft-dependent DCC and IN $\alpha6\beta4$ are important to prevent cell death, our results strongly suggest that lipid raft-independent DCC, as well as lipid raft-dependent IN $\alpha6\beta4$ are the key mediators in Ntn-1-induced cytoprotection in hypoxia-induced UCB-MSC apoptosis.

A critical matter with respect to the diverse functions of Ntn-1 is its signaling pathway involvement in cytoprotective effects, as mediated by the activation of survival signaling molecules via the alteration of Ntn receptor-dependent molecule complex.[27] Based on our results, Ntn-1 upregulated APPL-1/Akt2 complex formation. These results are supported by previous studies in which DCC-dependent signaling stimulated APPL-1/Akt2 complex formation,[28,29] and therefore, might be able to activate Akt2, thereby partially contributing to the anti-apoptotic effect.[29] However, Ntn-1 did not affect the DCC/caspase-3 complex in the plasma membrane of UCB-MSCs. Although the precise mechanisms that lead to Ntn-1-related anti-apoptotic protein complex

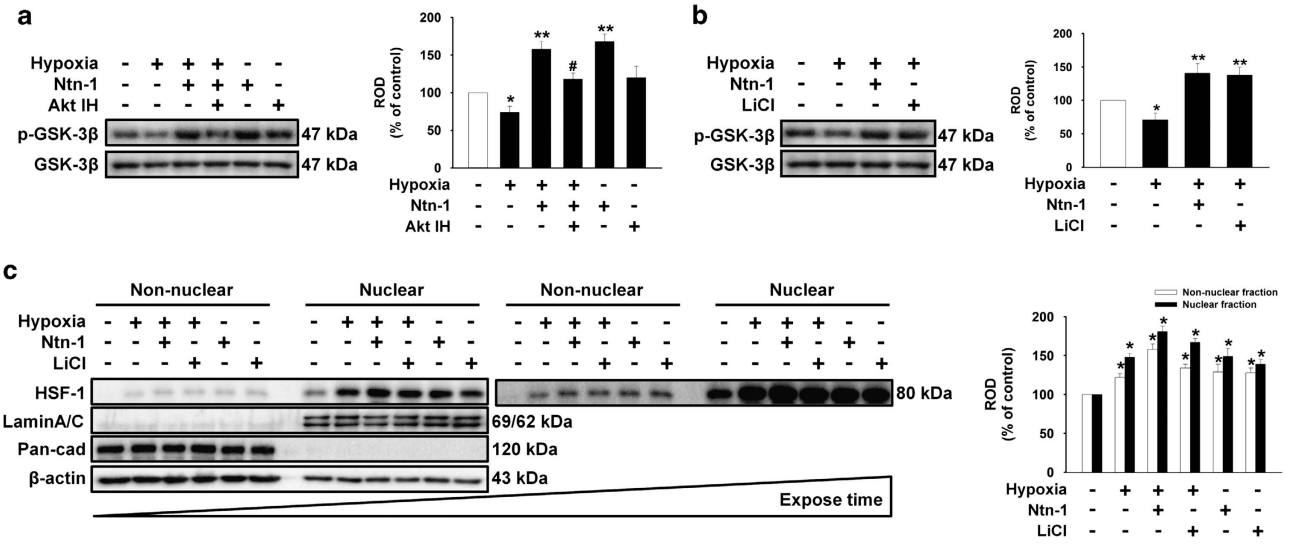

Figure 4 Involvement of GSK-3β/HSF-1-dependent HSP expression. (**a**) Cells were pretreated with Ntn-1 (10 ng/ml) and/or Akt inhibitor (10 μM) for 30 min before being exposed to hypoxia for 72 h; phospho-GSK-3β and GSK-3β were detected by western blot. (**b**) Cells were pretreated with Ntn-1 or LiCl (10 mM) for 30 min before being exposed to hypoxia for 72 h; phospho-GSK-3β and GSK-3β were detected by western blot. (**c**) Cells were pretreated with Ntn-1 or LiCl (10 mM) for 30 min before being exposed to hypoxia, and HSF-1, lamin A/C, pan-cadherin, and β-actin in the nuclear and non-nuclear fraction were detected by western blot. Each of the examples (**a**–**c**) is representative of four independent experiments. The right part (**a**–**c**) depicting the bars denotes the mean ± S.E. of four independent experiments for each condition determined from densitometry relative to β-actin or total GSK-3β. $^{*}P<0.05$ *versus* control, $^{**}P<0.05$ *versus* hypoxia alone, $^{\#}P<0.05$ *versus* combination of hypoxia and Ntn-1. ROD, relative optical density

dissociation or -association remain obscure, our results suggest that DCC-dependent APPL-1/Ak2 complex signaling is required for Ntn-1-stimulated anti-apoptotic effects in UCB-MSCs. However, this DCC-dependent APPL-1/Akt2 complex is simply not sufficient to fully explain cytoprotection, and the identification of other anti-apoptotic molecules is still required. Recent studies have shown that Ntn-1/Ntn receptor interaction especially enhances signaling, regulating the levels of phosphorylated Akt, which regulates various cell functions, including proliferation, motility, development, and survival.[30] Many studies have implicated the INs-mediated PI3K/Akt pathway in cell protection under various stresses[31,32] and in negatively regulating Bax.[33] Thus, we assumed that Ntn receptor-dependent Akt phosphorylation is also important for cytoprotection in UCB-MSCs. Our results show that Ntn-1 stimulated Akt phosphorylation, which was inhibited by DCC- and IN $\alpha6\beta4$ function-blocking antibodies. The present findings suggest that DCC- and IN $\alpha6\beta4$-dependent APPL-1/Ak2 complex and Akt signaling have important roles in Ntn-1-mediated cytoprotection, although DCC and/or INs are dependent on other signals, such as Erk and NF-κB pathways, which have an effect on cell survival and protection.[34,35]

GSK-3β exists downstream of Akt and regulates many related transcription factors, including HSF in several cell types.[36] Consistent with previous findings reported for human erythroid progenitors and muscle progenitor cells,[37,38] we observed a significant increase in anti-apoptotic protein levels, and decrease in pro-apoptotic protein levels, when GSK-3β was inactivated by Ntn. In addition, GSK-3β has a key role in increasing the levels of the HSF family, which enhances its cytoprotective effect.[39] In this context, we investigated the role of GSK-3β/HSF-1 on Ntn-1 effects in hypoxia-induced UCB-MSC apoptosis. We found that Akt inhibitor reduces Ntn-1-induced GSK-3β phosphorylation, and LiCl upregulates Ntn-1-induced HSF-1 expression. These results are supported by previous studies, which reveal that GSK-3β-dependent signaling stimulates HSF-1 expression and translocation in the nucleus.[39] Based on these results, as well as our own, we suggest the possibility that Ntn-1-induced GSK-3β phosphorylation upregulates the HSF-1-dependent signal.

Previous studies have shown that HSP isoforms, which are regulated by HSF, are implicated in maintaining cellular homeostasis and providing cellular defense by inhibition of various apoptotic signaling, or by the maintenance of survival signaling.[40] Among the HSP isoforms, it is well known that HSP27, HSP60, HSP70, and HSP90 are the key factors responsible for the protection of cellular damage.[40] Interestingly, in human endothelial cells, HSP isoform mRNA and protein expression were upregulated by hypoxia or ischemic injury.[41] In this study, we found that hypoxia and Ntn-1 promote HSP27 expression, but not HSP60, HSP70, or HSP90 expression. In addition, it was observed that *HSF-1*-specific siRNA only prevented an Ntn-1-induced increase of HSP27 expression, which suggests that the Ntn-1-induced increase of HSP27 expression is HSF-1-dependent in UCB-MSCs. Although HSF-1 regulated other HSP isoforms,[40] this discrepancy of these results might due to differences in species, cell types, or experimental conditions. Moreover, in this context, we investigated the role of Ntn-1-induced HSP27 on apoptotic signal transduction pathways. We found that *HSP27*-specific siRNA attenuated Ntn-1-induced Akt phosphorylation, and that Akt inhibitor prevented Ntn-1-reduced Bax expression. These results are supported by previous studies in which HSP27 inhibited Bax expression via PI3K-dependent mechanism in human

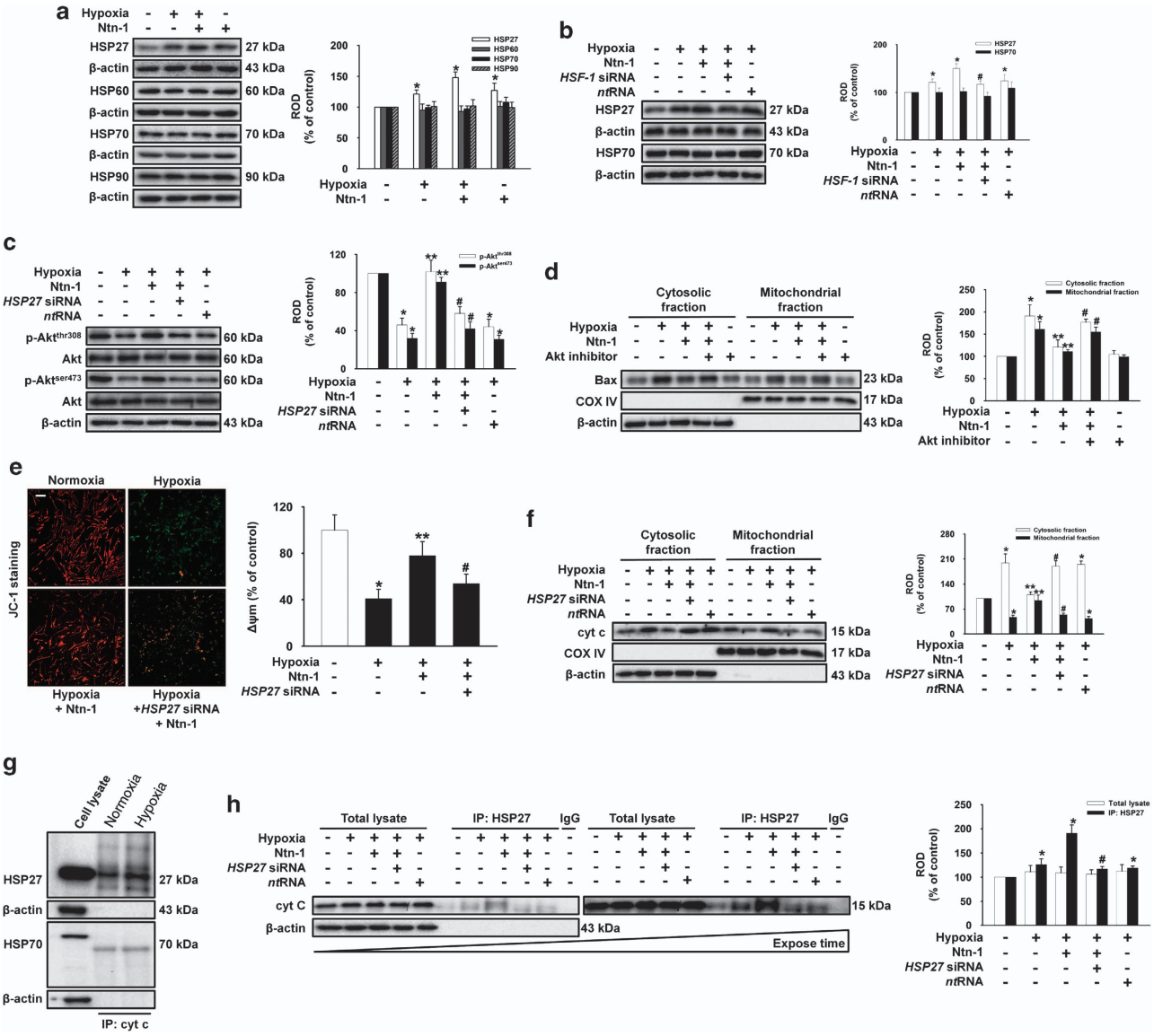

Figure 5 Role of HSP27 in Ntn-1-induced cytoprotective effects. (**a**) Cells were treated with Ntn-1 (10 ng/ml) for 30 min before hypoxia exposure for 72 h, and then HSP27, HSP60, HSP70, and HSP90 were detected by western blot. (**b and c**) Cells were transfected for 24 h with either *HSF-1*- or *HSP27*-specific siRNA (100 nmol/l) or *non-targeting* control siRNA (100 nmol/l) using Hyperfectamine prior to hypoxia with Ntn-1 exposure for 72 h. HSP27, HSP70, phospho-Akt^{thr308}, phospho-Akt^{ser473}, and Akt expressions were analyzed using western blot. (**d**) Cells were pretreated with Ntn-1 (10 ng/ml) and/or Akt inhibitor (10 μM) for 30 min before being exposed to hypoxia, and Bax, COX IV, and β-actin in the cytosolic and mitochondrial fraction were detected by western blot. (**e**) Acquisition of JC-1 fluorescence images of mitochondria was performed using confocal microscopy. Quantification of mitochondrial membrane potential is expressed as a ratio of J-aggregate to JC-1 monomer fluorescence intensity. Values are expressed as the mean ± S.E. of four independent experiments with triplicate measurement in one sample. *$P<0.05$ *versus* control, **$P<0.05$ *versus* hypoxia alone, $^{\#}P<0.05$ *versus* combination of hypoxia and Ntn-1. (**f**) Cells were pretreated with *HSP27*-specific siRNA or *non-targeting* control siRNA for 24 h prior to hypoxia with Ntn-1 exposure for 72 h and then harvested. Cyt *c*, COX IV, and β-actin in the cytosolic and mitochondrial fraction were detected by western blot. (**g**) Cells were exposed to hypoxia for 72 h and then immunoprecipitation of anti-cyt *c* was analyzed by western blotting with antibodies that recognize HSP27 or HSP70. (**h**) Cells were pretreated with *HSP27*-specific siRNA or *non-targeting* control siRNA for 24 h prior to hypoxia, with Ntn-1 exposure for 72 h and then harvested. Cell lysates were analyzed by western blotting with antibody to cyt *c*. Anti-HSP27 immunoprecipitation was analyzed by western blotting with cyt *c* antibody. Each of the examples (**a–d and f–g**) is representative of five independent experiments. The right part (**a–d** and **f–g**) depicting the bars denotes the mean ± S.E. of five independent experiments for each condition determined from densitometry relative to β-actin or total Akt. *$P<0.05$ *versus* control, **$P<0.05$ *versus* hypoxia alone, $^{\#}P<0.05$ *versus* combination of hypoxia and Ntn-1. ROD, Relative Optical Density

embryonic kidney cells.[42] In addition, we found that Ntn-1 significantly inhibited the hypoxia-induced loss of mitochondrial membrane potential and cyt *c* release in mitochondria. Moreover, Ntn-1 increases cyt *c* and HSP27 complex formation, which is inhibited by *HSP27*-specific siRNA. These results are consistent with previous studies, which have suggested that HSP27 might inhibit cyt *c* release by specifically interacting with mitochondria or interfering with apoptosome formation.[43,44] The present result demonstrated that Ntn-1-related HSP27 is a key factor involved in the

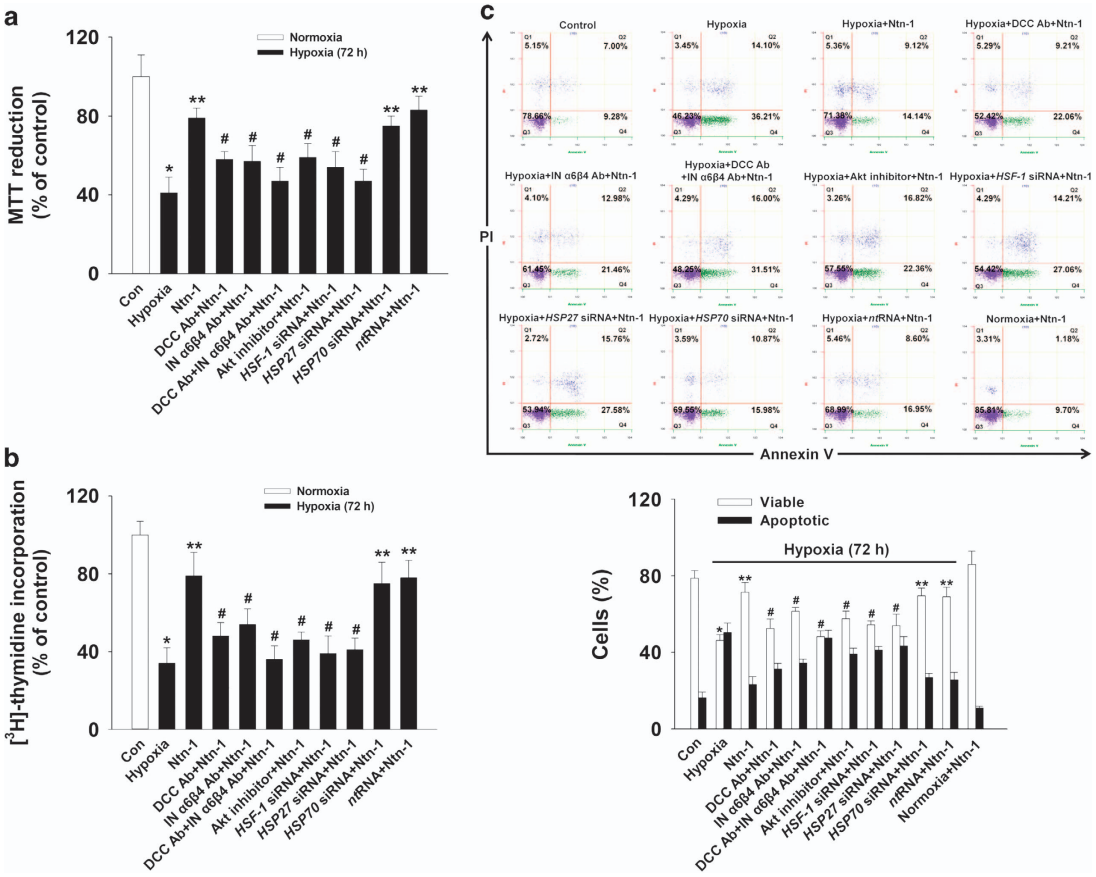

Figure 6 Involvement of DCC, IN $\alpha6\beta4$, Akt, GSK-3β, HSF-1, HSP27, and HSP70 on Ntn-1-induced protection of apoptosis in hypoxic condition. Cells were pretreated with DCC- and IN $\alpha6\beta4$ function-blocking antibodies, combination of DCC and IN $\alpha6\beta4$ function-blocking antibodies, Akt inhibitor, *HSF-1*-, *HSP27*-, *HSP70*-specific siRNA, and *non-targeting* control siRNA for 30 min or 24 h prior to hypoxia with Ntn-1 exposure for 72 h. (**a**) Cells were analyzed for their viability by MTT assay. The values are reported as a mean ± S.E. of three independent experiments with triplicate dishes. $^{*}P<0.05$ *versus* control, $^{**}P<0.05$ *versus* hypoxia alone, $^{\#}P<0.05$ *versus* combination of hypoxia and Ntn-1. (**b**) Cells were incubated with 1 μCi of [^{3}H]-thymidine for 1 h prior to counting. The values are reported as a mean ± S.E. of three independent experiments with triplicate dishes. $^{*}P<0.05$ *versus* control, $^{**}P<0.05$ *versus* hypoxia alone, $^{\#}P<0.05$ *versus* combination of hypoxia and Ntn-1. (**c**) Survival and apoptosis was measured using annexin V/PI staining and flow cytometry. Annexin V/PI double negative cells (Q3) were considered alive, annexin V-positive/PI-negative cells (Q4) were considered early apoptotic, and annexin V/PI double-positive cells (Q2) were considered late apoptotic. One representative experiment out of three is shown (top column). Quantitative analysis of the percentage of viable or apoptotic cells by FACS analysis (bottom column). $^{*,\#}P<0.05$ *versus* control, $^{**}P<0.05$ *versus* hypoxia alone. ROD, Relative Optical Density

inhibition of hypoxia-induced UCB-MSC apoptosis through the blockage of cyt *c* release in mitochondria and/or inhibition of Bax expression. Taken together, our results show that within the broader range of Ntn-1 receptor, intracellular signaling to regulate pro- and anti-apoptotic proteins through the HSF-1 and HSP27 cascade is important to generate Ntn-1-dependent protective strategies of hypoxia-induced UCB-MSC apoptosis (Figure 7). Therefore, identifying the mechanistic basis of Ntn receptor-mediated HSP27 by Ntn-1 may offer important insights into better understand the role of Ntn-1 in hypoxic injury, and therefore, might be a powerful tool or a potential therapeutic candidate for modulating UCB-MSC functions, as well as future tissue-regenerative strategies. In conclusion, Ntn-1 stimulates HSP27 expression through DCC- and IN $\alpha6\beta4$-dependent APPL-1, Akt, GSK-3β, and HSF-1 signaling pathways, thereby partially contributing to the protection of hypoxia-induced UCB-MSC apoptosis via the inhibition of mitochondrial dysfunction.

Materials and Methods

Materials. UCB-MSCs were obtained from the Obstetrics of College medicine, Chosun National University (Gwangju, Korea). Fetal bovine serum (FBS) was purchased from BioWhittaker Inc. (Walkersville, MO, USA). Ascorbic acid (vitamin C), lithium chloride, and NAC were obtained from Sigma Chemical Company (St. Louis, MO, USA). Anti-Akt2, APPL-1, Bax (6A7), Bcl-2, β-actin, caveolin-1, caveolin-2, caspase-3, caspase-9, cyt *c*, flotillin-2, GSK-3β, HIF-1α, HSF-1, HSP27, HSP60, HSP70, HSP90, IgG, integrin $\alpha6$, integrin $\beta4$, lamin A/C, pan-cadherin, phospho-Akt^{thr308}, phospho-Akt^{ser473}, phospho-GSK-3β, and total-Akt antibodies were purchased from Santa Cruz Biotechnology (Santa Cruz, CA, USA). Akt inhibitor and DCC antibody were purchased from Calbiochem (La Jolla, CA, USA). Cox IV antibody was purchased from Abcam (Cambridge, UK). Recombinant human Ntn-1 was purchased from R&D Systems (Minneapolis, MN, USA). [^{3}H]-thymidine was obtained from Dupont/NEN (Boston, MA, USA). Horseradish peroxidase (HRP)-conjugated goat anti-mouse and goat anti-rabbit IgG were purchased from Jackson ImmunoResearch (West Grove, PA, USA). Liquiscint was obtained from National Diagnostics (Parsippany, NJ, USA). FITC Annexin V Apoptosis Detection Kit I was purchased from BD Pharmingen (Franklin Lakes, NJ, USA). All other reagents were of the highest purity commercially available and were used as received.

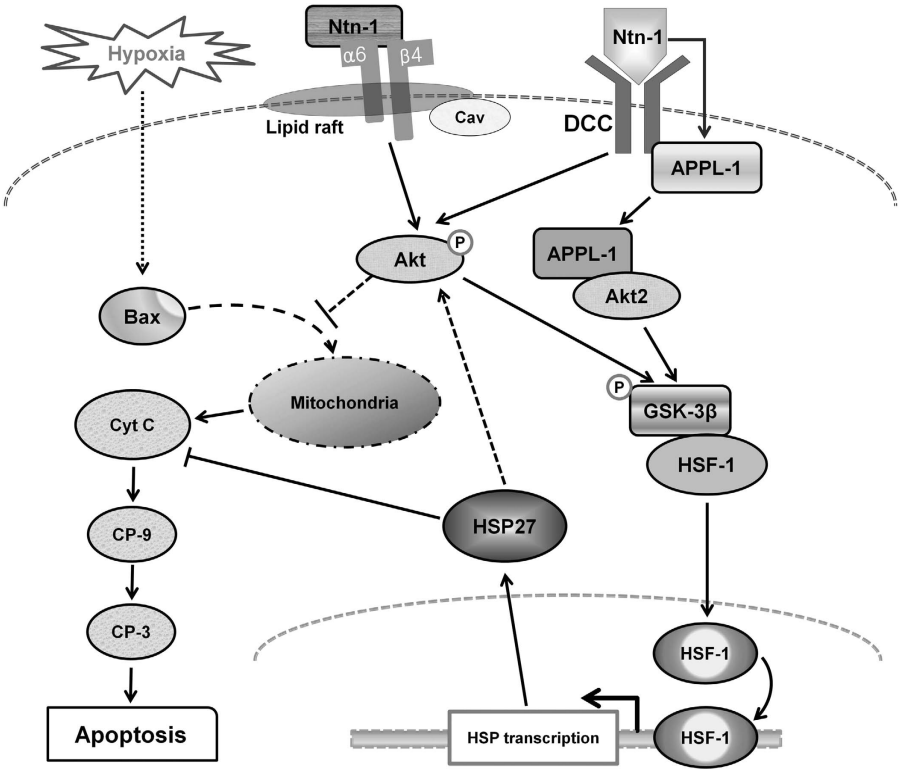

Figure 7 Hypothetical model of Ntn-1-related anti-apoptotic effect. Ntn-1 increased APPL-1/Akt2 complex formation and Akt phosphorylation via lipid raft-independent DCC and -dependent IN $\alpha6\beta4$. This signal increased GSK-3β phosphorylation and HSF-1 expression, and subsequently increased HSP27 expression. Finally, Ntn-1-induced HSP27 inhibited Bax expression and cyt *c* release thereby contributing to the protecting of hypoxia-induced UCB-MSC apoptosis

Isolation and characterization of human UCB-MSCs. The isolation and characterization of human UCB-MSCs were performed by cell surface marker analysis and multilineage differentiation in our previous report.[45] After the initial 31 days of primary culture, UCB-MSCs adhered to a plastic surface and presented a small population of single cells with a spindle shape. On days 7–10 after the initial plating, cells had the appearance of long, spindle-shaped fibroblastic cells, began to form colonies, and became confluent. After being subcultured, the structure of fibroblast-like cells appeared polygonal or spindly with a long process (appearance and growth of fibroblast-like hMSC colonies on the 31st day of culture as well as hMSCs at passages 4 and 12 of culture before multilineage differentiation). UCB-MSC passages 4–12 were observed under a microscope. Cells appeared normal on the basis of typical morphology. UCB-MSCs were positive for CD29, CD44, CD73, CD90, CD105, and HLA-ABC, but negative for CD14, CD34, CD45, CD74, CD106, and HLA-DR. With osteogenic supplementation, differentiation was apparent after 1 week of incubation. By the end of the second week, a portion of UCB-MSC became von Kossa-positive. Similarly, the portion of cells that was induced with adipogenic medium contained numerous oil red-O-positive lipid droplets. With neuronal supplementation, differentiation was apparent after 1 week of incubation. After 1 week, media were observed under a microscope to check for axon formation and enlargement of nuclei (all data not shown).

Culture of UCB-MSCs. UCB-MSCs were cultured without a feeder layer in phenol-red-free Dulbecco's modified Eagle's medium (DMEM; Gibco-BRL, Gaithersburg, MD, USA) supplemented with 3.7 g/l sodium bicarbonate, 1% penicillin and streptomycin, 1.7 mM L-glutamine, 0.1 mM β-mercaptoethanol, and 10% FBS. For each experiment, cells were grown in wells of 6- and 12-well plates, and in 35, 60, or 100-mm diameter culture dishes in an incubator maintained at 37 °C with 5% CO_2. The medium was replaced with serum-free DMEM at least 24 h before exposure to hypoxia. Following incubation, the cells were washed twice with phosphate-buffered saline (PBS) and then maintained in a serum-free DMEM including all supplements and indicated agents.

Hypoxic treatment of UCB-MSCs. UCB-MSCs were washed twice with PBS, and the medium was exchanged with fresh DMEM. Experiments were performed in a modular incubator chamber (Billups-Rotheberg, Del Mar, CA, USA) at 37 °C for 30 min under normoxic (92.3% air and 5.5% CO_2) or hypoxic (2.2% O_2, 5.5% CO_2, and 92.3% N_2) conditions at a flow rate of 20 l/min. The chamber was purged with gas, sealed, and placed in a conventional incubator at 37 °C. In this study, Ntn-1 did not affect HIF-1α protein expression level (Supplementary Figure 2). We determined hypoxic efficacy using HIF-1α antibody (Supplementary Figure 2).

[^{3}H]-thymidine incorporation. [^{3}H]-thymidine incorporation experiments were carried out as previously described.[46] In this study, the cells were cultured in a single well until they reached 70% confluence. They were then washed twice with PBS and maintained in serum-free DMEM including all supplements. After 24 h incubation, the cells were washed twice with PBS and incubated with fresh serum-free DMEM containing all the supplements and indicated agents. After the indicated incubation period, 1 μCi of [methyl-^{3}H]-thymidine was added to the cultures. Incubation with [^{3}H]-thymidine continued for 1 h at 37 °C. The cells were washed twice with PBS, fixed in 10% trichloroacetic acid (TCA) at 23 °C for 30 min, and then washed twice with 5% TCA. The acid-insoluble material was dissolved in 2 N NaOH for 12 h at 23 °C. Aliquots were removed to measure the radioactivity using a liquid scintillation counter. All values are reported as the mean ± S.E. of triplicate experiments. The values were converted from absolute counts to a percentage of the control in order to allow the comparison between experiments.

3-(4,5,-Dimethyl thiazolyl-2)-2,5-diphenyl tetrazolium bromide (MTT). UCB-MSCs were harvested after hypoxic condition for various periods (0–72 h). A total of 300 μl MTT reagent (Sigma) was added to each well 2 h prior to harvest. The supernatant was then removed and incubated with 400 μl dimethylsulfoxide (Sigma) for 10 min. Absorbance at 540 nm was recorded using an enzyme-linked immunosorbent assay-plate reader.

Cell number and viability assay. The cells were pretreated with Ntn-1 (10 ng/ml) for 30 min before being exposed to hypoxia for 72 h and washed twice with PBS. The cells were then detached from the culture dishes utilizing a 0.05% trypsin and 0.5 mM EDTA solution, and the detachment was quenched with Soybean trypsin inhibitor (0.05 mg/ml). Subsequently, 0.4% (w/v) trypan blue solution (500 μl) was added to the cell suspension, and the dead, live, and total cells were counted using Countess automated cell counter (Invitrogen, Carlsbad, CA, USA).

Fluorescence-activated cell sorter (FACS) analysis. The cells were pretreated with Ntn-1 (10 ng/ml) for 30 min before being exposed to hypoxia for 72 h. They were then dissociated in trypsin/EDTA pelleted by centrifugation. The cells were resuspended and washed twice at $\sim 10^6$ cells/ml in PBS containing 0.1% bovine serum albumin (BSA). Next, the cells were resuspended in 1 $\times$ Binding Buffer, and then stained with 5 μl of FITC Annexin V and 5 μl of PI, which were included in the FITC Annexin V Apoptosis Detection Kit I (BD Pharmingen). Then cells were at 25 °C for 15 min in the dark. The stained cells were analyzed by flow cytometry (Beckman Coulter, Fullerton, CA, USA). At least 10^4 events were recorded for each sample. The samples were analyzed using CXP software (Beckman Coulter).

Gene silencing with siRNA. UCB-MSCs were grown until 75% of the surface of the plate was covered, after which they were transfected for 24 h with either an siRNA specific for *HSF-1* (100 nmol/l; Santa Cruz Biotechnology; sc-35611), *HSP27* (100 nmol/l; Santa Cruz Biotechnology; sc-29350), *HSP70* (100 nmol/l; Dharmacon, Lafayette, CO, USA; L-065710-00) or a *non-targeting* siRNA as a negative control (100 nmol/l; Dharmacon; D-001206-13-20) with Hyperfectamine (QIAGEN, Valencia, CA, USA), according to the manufacturer's instructions. In this study, we determined each siRNA efficacy and effect of basal level, respectively (Supplementary Figure 3).

Cell fractionation. For fractionation of cells into cytosolic, membrane and nuclear fractions, we used a digitonin fractionation method that was described previously.[47,48] UCB-MSCs were serum-starved for 24 h, and then pretreated with or without Ntn-1 (10 ng/ml) for various periods (0–72 h) under hypoxic condition. The cells were then washed with PBS, and 20 μg/ml digitonin (Sigma) was added to permeabilize the cells. The cells were kept at 25 °C for 5 min and then on ice for an additional 30 min to allow the cytosol to diffuse into the buffer. The buffer was recovered and designated as the cytosolic fraction. The remainder of the cells were lysed with lysis buffer, scraped from the plastic, and centrifuged at 15 800 $\times$ *g* for 15 min. The supernatant was designated as the membrane fraction, and the pellet as the nuclear fraction. The nuclear fraction was resuspended in PBS, sonicated, and centrifuged to remove undissolved material.

RNA isolation and reverse transcription-polymerase chain reaction (RT-PCR). Total RNA was extracted from UCB-MSCs using STAT-60, which is a monophasic solution of phenol and guanidine isothiocyanate purchased from Tel-Test, Inc. (Friendswood, TX, USA). Reverse transcription (RT) was carried out using 3 μg of RNA using a RT system kit (Bioneer, Daejeon, Korea) with oligo(dT)18 primers. A PCR kit (Bioneer) was used to amplify 5 μl of the RT product under the following conditions: denaturation at 94 °C for 5 min, 30 cycles at 94 °C for 45 s, annealing temperature (Table 1) for 30 s, and 72 °C for 30 s, followed by 5 min of extension at 72 °C. Amplifications of *DCC, UNC5A, UNC5B, UNC5C,* and *Neogenin* cDNA were performed in UCB-MSCs, using the primers described in Table 1. PCR of *β-actin* was also performed as a control for RNA quantity.

Immunoprecipitation. Immunoprecipitation lysates were incubated with appropriate antibody and protein A-sepharose beads with gentle shaking overnight. Samples were washed thrice with lysis buffer and analyzed by sodium dodecyl sulfate polyacrylamide gel electrophoresis (SDS-PAGE). Bands were visualized with an enhanced chemiluminescence kit (Amersham Pharmacia Biotech Inc., Buckinghamshire, UK) and quantified with TINA 2.09 software (DesignSoft, Budapest, Hungary).

Western blot analysis. Cells were harvested, washed twice with PBS, and lysed with buffer (20 mM Tris (pH 7.5), 1 mM EDTA, 1 mM EGTA, 1% Triton X-100, 1 mg/ml aprotinin, and 1 mM phenylmethylsulfonylfluoride (PMSF)) for 30 min on ice. The lysates were then cleared by centrifugation (22 250 $\times$ *g* at 4 °C for 10 min). Protein concentration was determined by the Bradford method.[49] Equal amounts of protein (20 μg) were resolved by 10% SDS-PAGE and transferred to a polyvinylidene fluoride (PVDF) membrane. After the blots were washed with TBST (tris-buffer solution-Tween-20) (10 mM Tris-HCl (pH 7.6), 150 mM NaCl, and 0.05% Tween-20), the membranes were blocked with 5% skim milk for 1 h and incubated with an appropriate primary antibody at the dilution recommended by the supplier. The membrane was then washed and primary antibodies were detected with a horseradish peroxidase-conjugated secondary antibody. The bands were visualized by enhanced chemiluminescence (Amersham Pharmacia Biotech Inc.). Densitometric analysis was performed using the TINA version 2.09 program package. The ratios between each treated- and control samples were calculated for each individual experiment and expressed as a percentage of controls.

Detergent-free purification of caveolin-rich membrane fraction. Caveolin-enriched membrane fractions were prepared as described previously.[50] Cells were washed twice with ice-cold PBS, scraped into 2 ml of 500 mM sodium carbonate (pH 11.0), transferred into a plastic tube, and homogenized with a Sonicator 250 apparatus (Branson Ultrasonic, Danbury, CT, USA) using three 20-s bursts. The homogenate was adjusted to 45% sucrose by the addition of 2 ml of 90% sucrose prepared in 2-(*N*-morpholino) ethanesulfonic acid (MES)-buffered solution, consisting of 25 mM MES-buffer solution (pH 6.5) and 0.15 M NaCl, and placed at the bottom of an ultracentrifuge tube. A 5–35% discontinuous sucrose gradient was formed (4 ml each of 5 and 35% sucrose, both in MES-buffer solution containing 250 mM sodium carbonate) and centrifuged at 40 000 r.p.m. for 20 h in a SW 41 Rotor (Beckman Coulter). Twelve fractions (1 ml each) were collected and analyzed by 10–12% SDS-PAGE.

Detection of mitochondrial membrane potential. Loss of the mitochondrial membrane potential ($\Delta\psi$) was assessed by using the fluorescent probe JC-1 (Molecular Probes, Eugene, OR, USA), which exists predominantly in the monomeric form in cells with depolarized mitochondria and is fluorescent

Table 1 Primers used for polymerase chain reaction

Gene	Identification	Primer sequence, 5′–3′	Annealing Temperature (°C)	Size (bp)	Ref.
DCC	Sense	CAAGTGCCCCGCCTCAGAACG	55	434	51
	Antisense	GCTCCCAACGCCATAACCGATAAT			
UNC5A	Sense	GCACAAGCCGGAAGACGTGAG	56	440	52
	Antisense	GCATCGTGGGTGTCATGCAGG			
UNC5B	Sense	CAAGGCAGAAAGTACCCTCCCGCT	56	420	52
	Antisense	CAGCACCTCCTTCAGTGCTAC			
UNC5C	Sense	GGCAGCAAGACAAGATCTGC	56	460	52
	Antisense	ATGGGTGGCCTCATAGTTTC			
Neogenin	Sense	CGCTACCTTTGAATTAGTTCCT	60	380	30
	Antisense	GATGATGTAACCTGTAATCTTGCC			
β-Actin	Sense	AGCCATGTACGTAGCCATCC	55	350	53
	Antisense	CTCTCAGCTGTGGTGGTGAA			

Abbreviations: DCC, deleted in colon cancer; Ref, references; *UNC5A*, uncoordinated-5-A; *UNC5B*, uncoordinated-5-B; *UNC5C*, uncoordinated-5-C

green at 490 nm. Cells with polarized mitochondria predominantly contain JC-1 in an aggregated form and are fluoresce reddish-orange. Cells were incubated with 5 μM JC-1 for 10 min at 37 °C, then washed and placed on a warmed microscope stage at 37 °C. Cells were viewed at $\times$600 magnification with a FluoView 300 confocal microscope. Fluorescence was excited at 488 nm, and emitted light was observed at 515–540 nm. To quantify the mitochondrial membrane potential, JC-1-treated cells were rinsed twice in ice-cold PBS and scraped off the surface. A 100-μl cell suspension was loaded into wells of a 96-well plate, and examined with a Victor3 luminometer (Perkin-Elmer Inc., Waltham, MA, USA) and a fluorescent plate reader, with excitation and emission wavelengths of 485 and 535 nm, respectively. The ratio of J-aggregate intensity to JC-1 monomer intensity for each region was calculated. A decrease in this ratio was interpreted as loss of $\Delta\psi$m, whereas an increase was interpreted as gain in $\Delta\psi$m.

Isolation of mitochondria. UCB-MSCs were serum-starved for 24 h, and then pretreated with or without Ntn-1 (10 ng/ml) for various periods (0–72 h) under hypoxic condition. The cells were then extracted using the PIERCE Mitochondria Isolation Kit for Cultured Cells (Thermo Fisher Scientific, Rockford, IL, USA) according to the manufacturer's instructions.

Statistical analysis. Results are expressed as means $\pm$ S.E. All experiments were analyzed by ANOVA, followed in some cases by a comparison of treatment means with the control using the Bonferroni–Dunn test. Differences were considered statistically significant at $P<0.05$.

Conflict of Interest

The authors declare no conflict of interest.

Acknowledgements. This study was supported by a grant of the Korean Health Technology R&D Project, Ministry of Health and Welfare, Republic of Korea (A120216), and a grant from the Next-Generation BioGreen 21 Program (No. PJ009090), Rural Development Administration, Republic of Korea.

1. Qiao C, Xu W, Zhu W, Hu J, Qian H, Yin Q *et al.* Human mesenchymal stem cells isolated from the umbilical cord. *Cell Biol Int* 2008; **32**: 8–15.
2. Sensebé L, Krampera M, Schrezenmeier H, Bourin P, Giordano R. Mesenchymal stem cells for clinical application. *Vox Sang* 2010; **98**: 93–107.
3. Wakitani S, Nawata M, Tensho K, Okabe T, Machida H, Ohgushi H. Repair of articular cartilage defects in the patello-femoral joint with autologous bone marrow mesenchymal cell transplantation: three case reports involving nine defects in five knees. *J Tissue Eng Regen Med* 2007; **1**: 74–79.
4. Zhu W, Chen J, Cong X, Hu S, Chen X. Hypoxia and serum deprivation-induced apoptosis in mesenchymal stem cells. *Stem Cells* 2006; **24**: 416–425.
5. Lee SH, Lee YJ, Han HJ. Role of hypoxia-induced fibronectin-integrin β1 expression in embryonic stem cell proliferation and migration: involvement of PI3K/Akt and FAK. *J Cell Physiol* 2011; **226**: 484–493.
6. Prado-Lopez S, Conesa A, Armiñán A, Martinez-Losa M, Escobedo-Lucea C, Gandia C *et al.* Hypoxia promotes efficient differentiation of human embryonic stem cells to functional endothelium. *Stem Cells* 2010; **28**: 407–418.
7. Lee SH, Suh HN, Lee YJ, Seo BN, Ha JW, Han HJ. Midkine prevented hypoxic injury of mouse embryonic stem cells through activation of Akt and HIF-1α via low-density lipoprotein receptor-related protein-1. *J Cell Physiol* 2012; **227**: 1731–1739.
8. Lai Wing Sun K, Correia JP, Kennedy TE. Netrins: versatile extracellular cues with diverse functions. *Development* 2011; **138**: 2153–2169.
9. Bayat M, Baluchnejadmojarad T, Roghani M, Goshadrou F, Ronaghi A, Mehdizadeh M. Netrin-1 improves spatial memory and synaptic plasticity impairment following global ischemia in the rat. *Brain Res* 2012; **1452**: 185–194.
10. Wu TW, Li WW, Li H. Netrin-1 attenuates ischemic stroke-induced apoptosis. *Neuroscience* 2008; **156**: 475–482.
11. Bradford D, Cole SJ, Cooper HM. Netrin-1: diversity in development. *Int J Biochem Cell Biol* 2009; **41**: 487–493.
12. Fitamant J, Guenebeaud C, Coissieux MM, Guix C, Treilleux I, Scoazec JY *et al.* Netrin-1 expression confers a selective advantage for tumor cell survival in metastatic breast cancer. *Proc Natl Acad Sci USA* 2008; **105**: 4850–4855.
13. Petit A, Sellers DL, Liebl DJ, Tessier-Lavigne M, Kennedy TE, Horner PJ. Adult spinal cord progenitor cells are repelled by netrin-1 in the embryonic and injured adult spinal cord. *Proc Natl Acad Sci USA* 2007; **104**: 17837–17842.
14. Xie H, Zou L, Zhu J, Yang Y. Effects of netrin-1 and netrin-1 knockdown on human umbilical vein endothelial cells and angiogenesis of rat placenta. *Placenta* 2011; **32**: 546–553.
15. Li Q, Yao D, Ma J, Zhu J, Xu X, Ren Y *et al.* Transplantation of MSCs in combination with netrin-1 improves neoangiogenesis in a rat model of hind limb ischemia. *J Surg Res* 2011; **166**: 162–169.
16. Xu B, Goldman JS, Rymar VV, Forget C, Lo PS, Bull SJ *et al.* Critical roles for the netrin receptor deleted in colorectal cancer in dopaminergic neuronal precursor migration, axon guidance, and axon arborization. *Neuroscience* 2010; **169**: 932–949.
17. Bernet A, Fitamant J. Netrin-1 and its receptors in tumour growth promotion. *Expert Opin Ther Targets* 2008; **12**: 995–1007.
18. Nikolopoulos SN, Giancotti FG. Netrin-integrin signaling in epithelial morphogenesis, axon guidance and vascular patterning. *Cell Cycle* 2005; **4**: e131–e135.
19. Yebra M, Montgomery AM, Diaferia GR, Kaido T, Silletti S, Perez B *et al.* Recognition of the neural chemoattractant Netrin-1 by integrins α6β4 and α3β1 regulates epithelial cell adhesion and migration. *Dev Cell* 2003; **5**: 695–707.
20. Bernadskaya YY, Wallace A, Nguyen J, Mohler WA, Soto MC. UNC-40/DCC, SAX-3/Robo, and VAB-1/Eph polarize F-actin during embryonic morphogenesis by regulating the WAVE/SCAR actin nucleation complex. *PLoS Genet* 2012; **8**: e1002863.
21. Krishna OD, Jha AK, Jia X, Kiick KL. Integrin-mediated adhesion and proliferation of human MSCs elicited by a hydroxyproline-lacking, collagen-like peptide. *Biomaterials* 2011; **32**: 6412–6424.
22. Sampath P, Pritchard DK, Pabon L, Reinecke H, Schwartz SM, Morris DR *et al.* A hierarchical network controls protein translation during murine embryonic stem cell self-renewal and differentiation. *Cell Stem Cell* 2008; **2**: 448–460.
23. Chen M, Sinha M, Luxon BA, Bresnick AR, O'Connor KL. Integrin α6β4 controls the expression of genes associated with cell motility, invasion, and metastasis, including *S100A4*/metastasin. *J Biol Chem* 2009; **284**: 1484–1494.
24. Herincs Z, Corset V, Cahuzac N, Furne C, Castellani V, Hueber AO *et al.* DCC association with lipid rafts is required for netrin-1-mediated axon guidance. *J Cell Sci* 2005; **118**: 1687–1692.
25. Nasarre P, Potiron V, Drabkin H, Roche J. Guidance molecules in lung cancer. *Cell Adh Migr* 2010; **4**: 130–145.
26. Whitsett JA, Kalinichenko VV. Integrin α6β4 defines a novel lung epithelial progenitor cell: a step forward for cell-based therapies for pulmonary disease. *J Clin Invest* 2011; **121**: 2543–2545.
27. Arakawa H. Netrin-1 and its receptors in tumorigenesis. *Nat Rev Cancer* 2004; **4**: 978–987.
28. Cirulli V, Yebra M. Netrins: beyond the brain. *Nat Rev Mol Cell Biol* 2007; **8**: 296–306.
29. Mitsuuchi Y, Johnson SW, Sonoda G, Tanno S, Golemis EA, Testa JR. Identification of a chromosome 3p14.3-21.1 gene, APPL, encoding an adapter molecule that interacts with the oncoprotein-serine/threonine kinase AKT2. *Oncogene* 1999; **18**: 4891–4898.
30. Wang W, Reeves WB, Ramesh G. Netrin-1 increases proliferation and migration of renal proximal tubular epithelial cells via the UNC5B receptor. *Am J Physiol Renal Physiol* 2009; **296**: F723–F729.
31. Faghiri Z, Bazan NG. PI3K/Akt and mTOR/p70S6K pathways mediate neuroprotectin D1-induced retinal pigment epithelial cell survival during oxidative stress-induced apoptosis. *Exp Eye Res* 2010; **90**: 718–725.
32. Miyamoto S, Murphy AN, Brown JH. Akt mediated mitochondrial protection in the heart: metabolic and survival pathways to the rescue. *J Bioenerg Biomembr* 2009; **41**: 169–180.
33. Gardai SJ, Hildeman DA, Frankel SK, Whitlock BB, Frasch SC, Borregaard N *et al.* Phosphorylation of Bax Ser^{184} by Akt regulates its activity and apoptosis in neutrophils. *J Biol Chem* 2004; **279**: 21085–21095.
34. Donthamsetty S, Mars WM, Orr A, Wu C, Michalopoulos GK. Protection against Fas-induced fulminant hepatic failure in liver specific integrin linked kinase knockout mice. *Comp Hepatol* 2011; **10**: 11.
35. Forcet C, Stein E, Pays L, Corset V, Llambi F, Tessier-Lavigne M *et al.* Netrin-1-mediated axon outgrowth requires deleted in colorectal cancer-dependent MAPK activation. *Nature* 2002; **417**: 443–447.
36. Jope RS, Johnson GV. The glamour and gloom of glycogen synthase kinase-3. *Trends Biochem Sci* 2004; **29**: 95–102.
37. Somervaille TC, Linch DC, Khwaja A. Growth factor withdrawal from primary human erythroid progenitors induces apoptosis through a pathway involving glycogen synthase kinase-3 and Bax. *Blood* 2001; **98**: 1374–1381.
38. Wang Y, Hao Y, Alway SE. Suppression of GSK-3β activation by M-cadherin protects myoblasts against mitochondria-associated apoptosis during myogenic differentiation. *J Cell Sci* 2011; **124**: 3835–3847.
39. Jones Q, Voegeli TS, Li G, Chen Y, Currie RW. Heat shock proteins protect against ischemia and inflammation through multiple mechanisms. *Inflamm Allergy Drug Targets* 2011; **10**: 247–259.
40. Sreedhar AS, Csermely P. Heat shock proteins in the regulation of apoptosis: new strategies in tumor therapy: a comprehensive review. *Pharmacol Ther* 2004; **101**: 227–257.
41. Kang MJ, Jung SM, Kim MJ, Bae JH, Kim HB, Kim JY *et al.* DNA-dependent protein kinase is involved in heat shock protein-mediated accumulation of hypoxia-inducible factor-1α in hypoxic preconditioned HepG2 cells. *FEBS J* 2008; **275**: 5969–5981.
42. Havasi A, Li Z, Wang Z, Martin JL, Botla V, Ruchalski K *et al.* Hsp27 inhibits Bax activation and apoptosis via a phosphatidylinositol 3-kinase-dependent mechanism. *J Biol Chem* 2008; **283**: 12305–12313.
43. Bruey JM, Ducasse C, Bonniaud P, Ravagnan L, Susin SA, Diaz-Latoud C *et al.* Hsp27 negatively regulates cell death by interacting with cytochrome c. *Nat Cell Biol* 2000; **2**: 645–652.

44. Samali A, Robertson JD, Peterson E, Manero F, van Zeijl L, Paul C *et al.* Hsp27 protects mitochondria of thermotolerant cells against apoptotic stimuli. *Cell Stress Chaperones* 2001; **6**: 49–58.
45. Yun SP, Lee MY, Ryu JM, Song CH, Han HJ. Role of HIF-1α and VEGF in human mesenchymal stem cell proliferation by 17β-estradiol: involvement of PKC, PI3K/Akt, and MAPKs. *Am J Physiol Cell Physiol* 2009; **296**: C317–C326.
46. Brett CM, Washington CB, Ott RJ, Gutierrez MM, Giacomini KM. Interaction of nucleoside analogues with the sodium-nucleoside transport system in brush border membrane vesicles from human kidney. *Pharm Res* 1993; **10**: 423–426.
47. Sørensen V, Zhen Y, Zakrzewska M, Haugsten EM, Wälchli S, Nilsen T *et al.* Phosphorylation of fibroblast growth factor (FGF) receptor 1 at Ser777 by p38 mitogen-activated protein kinase regulates translocation of exogenous FGF1 to the cytosol and nucleus. *Mol Cell Biol* 2008; **28**: 4129–4141.
48. Wiedłocha A, Nilsen T, Wesche J, Sørensen V, Małecki J, Marcinkowska E *et al.* Phosphorylation-regulated nucleocytoplasmic trafficking of internalized fibroblast growth factor-1. *Mol Biol Cell* 2005; **16**: 794–810.
49. Bradford MM. A rapid and sensitive method for the quantitation of microgram quantities of protein utilizing the principle of protein-dye binding. *Anal Biochem* 1976; **72**: 248–254.
50. Song KS, Li S, Okamoto T, Quilliam LA, Sargiacomo M, Lisanti MP. Co-purification and direct interaction of Ras with caveolin, an integral membrane protein of caveolae microdomains. Detergent-free purification of caveolae microdomains. *J Biol Chem* 1996; **271**: 9690–9697.
51. Shekarabi M, Kennedy TE. The netrin-1 receptor DCC promotes filopodia formation and cell spreading by activating Cdc42 and Rac1. *Mol Cell Neurosci* 2002; **19**: 1–17.
52. Rodrigues S, De Wever O, Bruyneel E, Rooney RJ, Gespach C. Opposing roles of netrin-1 and the dependence receptor DCC in cancer cell invasion, tumor growth and metastasis. *Oncogene* 2007; **26**: 5615–5625.
53. Jang MW, Yun SP, Park JH, Ryu JM, Lee JH, Han HJ. Cooperation of Epac1/Rap1/Akt and PKA in prostaglandin E_2 -induced proliferation of human umbilical cord blood derived mesenchymal stem cells: involvement of c-Myc and VEGF expression. *J Cell Physiol* 2012; **227**: 3756–3767.

Supplementary Information accompanies this paper on Cell Death and Disease website (http://www.nature.com/cddis)